Received: 26 March 2024 | Accepted: 30 September 2024

DOI: 10.1002/aps3.11629

Applications in Plant Sciences

APPLICATION ARTICLE

The sensitivity of reconstructed carbon dioxide concentrations to stomatal preparation methods using a leaf gas exchange model

Michael D. Machesky[1,2] | **Nathan D. Sheldon**[1] | **Michael T. Hren**[3] | **Selena Y. Smith**[1]

[1]Department of Earth and Environmental Sciences, University of Michigan, 1100 N. University Ave., Ann Arbor, Michigan 48109, USA

[2]Harvard University Herbaria, 22 Divinity Ave., Cambridge, Massachusetts 02138, USA

[3]Department of Earth Sciences, University of Connecticut, 354 Mansfield Rd., Storrs, Connecticut 06269, USA

Correspondence

Selena Y. Smith, Department of Earth and Environmental Sciences, University of Michigan, 1100 N. University Ave., Ann Arbor, Michigan 48109, USA.
Email: sysmith@umich.edu

Abstract

Premise: Mechanistic models using stomatal traits and leaf carbon isotope ratios to reconstruct atmospheric carbon dioxide (CO_2) concentrations (c_a) are important to understand the Phanerozoic paleoclimate. However, methods for preparing leaf cuticles to measure stomatal traits have not been standardized.

Methods: Three people measured the stomatal density and index, guard cell length, guard cell pair width, and pore length of leaves from the same *Ginkgo biloba*, *Quercus alba*, and *Zingiber mioga* leaves growing at known CO_2 levels using four preparation methods: fluorescence on cleared leaves, nail polish, dental putty on fresh leaves, and dental putty on dried leaves.

Results: There are significant differences between trait measurements from each method. Modeled c_a calculations are less sensitive to method than individual traits; however, the choice of assumed carbon isotope fractionation also impacted the accuracy of the results.

Discussion: We show that there is not a significant difference between c_a estimates made using any of the four methods. Further study is needed on the fractionation due to carboxylation of ribulose bisphosphate (RuBP) in individual plant species before use as a paleo-CO_2 barometer and to refine estimates based upon widely applied taxa (e.g., *Ginkgo*). Finally, we recommend that morphological measurements be made by multiple observers to reduce the effect of individual observational biases.

KEYWORDS

Ginkgo, paleobotany, paleoclimate, *Quercus*, stable isotopes, stomata, *Zingiber*

Because plants interact directly with the atmosphere through photosynthesis, living and fossil leaves are useful as recorders of the environmental conditions in which they grew through both morphological and chemical traits (McElwain, 2018). Some of the most well-studied leaf traits for paleoclimate are from stomata, i.e., the pores on leaf surfaces that regulate gas exchange. Stomata are found on all extant and fossil land plants except for liverworts and are well preserved across the fossil record. Today, they are most commonly located on the abaxial surface of leaves (McElwain and Steinthorsdottir, 2017). Especially useful for paleoatmospheric reconstruction is the stomatal index (*SI*) of a plant, i.e., the ratio of stomata to the total number of epidermal cells on the bottom of a leaf. Unlike stomatal density (*SD*; the number of stomata per unit area), *SI* is not affected by environmental factors such as temperature, water availability, and irradiance and can therefore be applied to carbon dioxide concentration (hereafter [CO_2]) reconstruction independently of other traits (McElwain and Chaloner 1995; Royer, 2001). Stomatal index correlates negatively with [CO_2] in taxon-dependent relationships in both modern and fossil leaves, because there are fewer stomata on plants' leaves when CO_2 is higher to

minimize water loss when CO_2 is not limiting (Royer, 2001; Rundgren and Beerling, 2003). More recently, models were developed to combine the use of *SD*, stomatal pore length, and carbon isotope ratio ($\delta^{13}C$) to refine [CO_2] estimates from fossil leaves (Franks and Beerling, 2009; Franks et al., 2014; Royer et al., 2019; Konrad et al., 2021; Steinthorsdottir et al., 2022).

Despite the usefulness of stomatal characteristics in paleoclimatic reconstruction, the method for preparing leaf cuticles to measure stomatal size and index is not standardized. Different methods of preparing the leaf cuticle impression could potentially yield results that vary significantly. Specifically, using dried rather than fresh leaves or a fossil may result in smaller stomatal measurements due to sample desiccation and resulting shrinkage or differential compaction. It is important to understand what differences exist between preparation methods for such a widely applied proxy, so that error can be accounted for. We tested whether four methods of leaf cuticle preparation produce comparable stomatal trait data when applied to the same leaves from three different species. We assessed *SD* and *SI*, guard cell length, guard cell pair width, and pore length of each sample using each of the four methods to see whether different methods yielded different results. We also tested whether such differences would be significant enough to alter mechanistic paleoclimate model estimates by comparing [CO_2] values calculated using a widely applied leaf gas exchange model (Franks et al., 2014) for each method.

METHODS

Sample collection

Leaves from *Ginkgo biloba* L. ($n = 16$), *Zingiber mioga* (Thunb.) Roscoe ($n = 28$), and *Quercus alba* L. ($n = 15$) were collected from Matthaei Botanical Gardens ($n = 12$, *G. biloba*) and the Arbor Hills neighborhood of Ann Arbor, Michigan, in autumn 2021 and 2022 (Figure 1). These plants were chosen because of their fossil record, ease of collection access, and the original taxon-specific calibrations of *G. biloba* and *Q. robur* L. from Franks et al. (2014) derived for use in their model. Additionally, these plants represent a diversity of growth forms and plant groups, as *G. biloba* is a gymnosperm tree, *Q. alba* a dicotyledonous tree, and *Z. mioga* a herbaceous monocot.

Stomatal analysis

The following four methods were used to obtain stomatal data:

1. Nail polish on fresh leaves: A single, thin layer of clear nail polish was applied to the abaxial surface of each leaf shortly after they were collected. The dried polish was transferred and adhered to a microscope slide by picking it up and sticking it to the slide with clear packing tape (Hilu and Randall, 1984).
2. Dental putty on fresh leaves (Porter et al., 2019): A cell-level impression of the cuticle of each leaf sample was made using AFFINIS light body surface-activated silicone-based dental putty (Coltène, Altstätten, Switzerland) on the abaxial surface of each leaf shortly after they were collected. Once dried, a layer of clear nail polish was applied to the putty mold and allowed to dry. The nail polish impression was then transferred and adhered to a microscope slide using clear packing tape.
3. Dental putty on dry leaves: The leaves were dried in a plant press for at least one week. Once fully dried, the process described in method 2 was repeated for each leaf.
4. Fluorescence on cleared leaves: To chemically clear each leaf, ~1-cm^2 portions from the center of leaves were digested using a 5% NaOH solution. Depending on the thickness of the leaf, this took anywhere from two days to two weeks. The leaves were then rinsed in water, bleached, rinsed again, and put through an ethanol dehydration series (50%, 70%, 100%). Samples were stained with 5% safranin–ethanol solution, washed with 70% ethanol, and given a final 100% ethanol bath before they were cleared and mounted in cedarwood oil between 0.05-inch acetate sheets sealed using aluminum tape.

Three different 0.069-mm^2 viewpoints of each sample were imaged using a Nikon Eclipse LV100ND microscope (Nikon, Tokyo, Japan). Fluorescence was used for the cleared leaves, while the other samples were imaged with transmitted light. Using the Cell Counter plug-in in ImageJ (Schneider et al., 2012), three counters independently measured stomatal traits in each image (counter 1: Michael D. Machesky [all], counter 2: Kelly D. Martin [all], counter 3: Kate M. Morrison [*Ginkgo*] or Katherine Harpenau [*Quercus*, *Zingiber*]) after first standardizing methodology by discussion and measuring three images together to ensure the same results. This allowed for the uncertainty associated with human error in cell counting and measurement to be quantified by comparing the differences between each person's measurements. For each image, we counted the number of stomata and epidermal cells to calculate *SI*, and measured the guard cell length, guard cell pair width, and pore length of three individual stomata using ImageJ (Schneider et al., 2012) (Figure 2). *SI* and *SD* were calculated using the following equations:

$$SI = 100 \times \frac{\#Stomata}{(\#Stomata + \#Epidermal\ Cells)} \quad (1)$$

$$SD = \frac{\#Stomata}{area\ in\ mm^2} \quad (2)$$

All data for stomatal analyses for each individual counter and the average of all counters' data are available in Appendix S1 (see Supporting Information with this article).

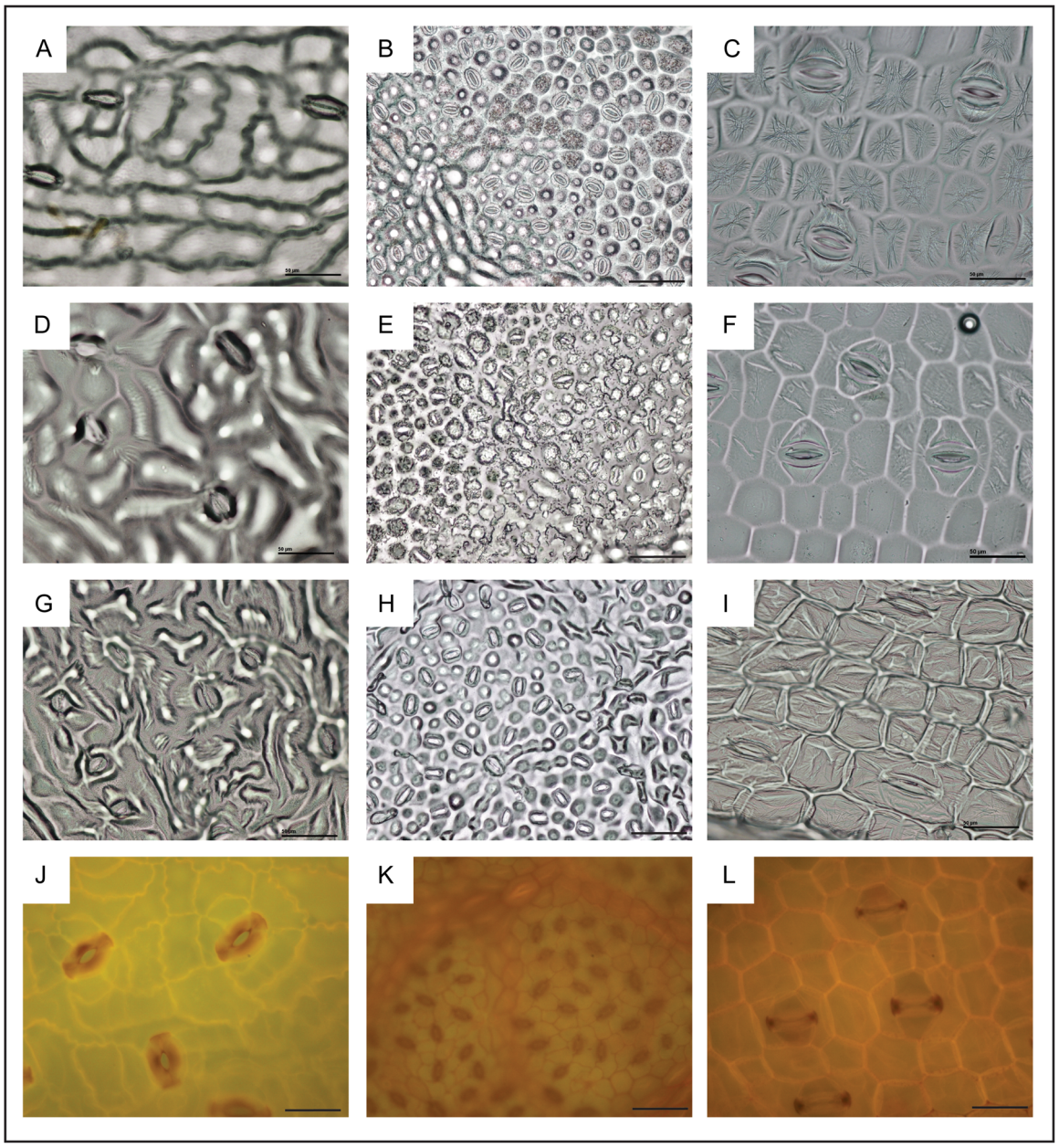

FIGURE 1 Light micrograph images of leaf cuticles of each species prepared using each method. (A, D, G, J) *Ginkgo biloba*, (B, E, H, K) *Quercus alba*, (C, F, I, L) *Zingiber mioga*. (A–C) Polish, (D–F) putty on fresh leaves, (G–I) putty on dried leaves, (J–L) cleared leaves under fluorescence. Scale bars = 50 μm.

Estimating c_a

Atmospheric [CO_2] (c_a) was calculated for each sample using the mechanistic model from Franks et al. (2014), herein referred to as the Franks model, and updates from Royer et al. (2019). The basis of this model is the relationship between c_a and leaf CO_2 assimilation rate (Farquhar and Sharkey, 1982; von Caemmerer, 2000) shown below as Equation 3:

$$c_a = \frac{A_n}{g_{c\,(tot)} \cdot (1 - c_i/c_a)} \quad (3)$$

where A_n is the CO_2 assimilation rate by leaves (μmol·m^{-2}·s^{-1}), $g_{c(tot)}$ is the total operational conductance to CO_2 diffusion from the atmosphere to sites of photosynthesis within the leaf (mol·m^{-2}·s^{-1}), and c_i/c_a is the ratio of the leaf internal CO_2 concentration (c_i) to that of the atmosphere. For the calculations, A_n values calculated as a function of modeled c_a from Franks et al. (2014) were used. A value of 8.09 μmol·m^{-2}·s^{-1} calculated for *G. biloba* by Kowalczyk et al. (2018) was used for *G. biloba*, and a value of 14.9 μmol·m^{-2}·s^{-1} calculated for *Q. robur* by Franks et al. (2014) was used for *Q. alba* and *Z. mioga*. *Quercus robur* was the only angiosperm for which an A_n value was calculated by Franks et al. and was therefore

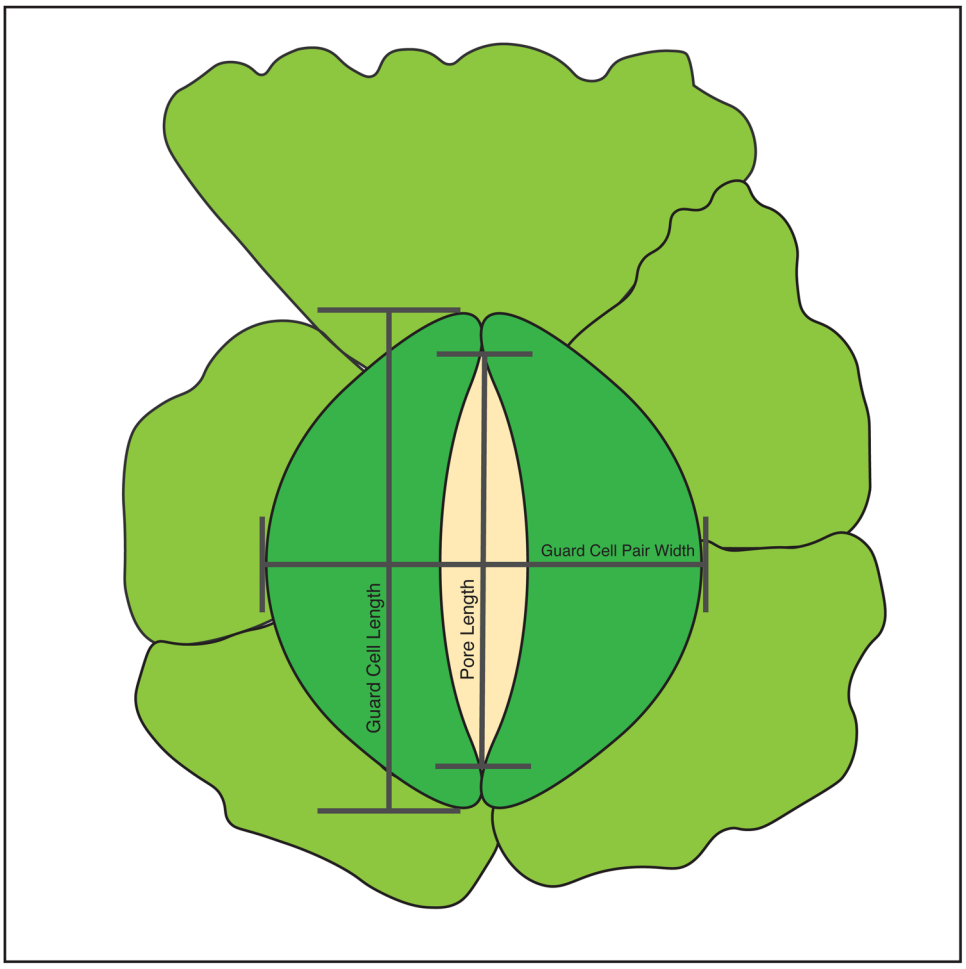

FIGURE 2 Diagram showing a stoma (beige), guard cells (darker green), five subsidiary cells (lighter green), and the three stomatal measurements taken (dark gray lines).

assumed to be the closest value for *Q. alba* and *Z. mioga*. $g_{c(tot)}$ is calculated using Equation 4:

$$g_{c\,(tot)} = \left(\frac{1}{g_{cb}} + \frac{1}{\zeta g_{c\,(\max)}} + \frac{1}{g_m} \right)^{-1} \quad (4)$$

where g_{cb} is the leaf boundary layer conductance to CO_2 ($mol{\cdot}m^{-2}{\cdot}s^{-1}$), g_m is the mesophyll conductance to CO_2 ($mol{\cdot}m^{-2}{\cdot}s^{-1}$), $g_{c(\max)}$ is the maximum operational stomatal conductance to CO_2 ($mol{\cdot}m^{-2}{\cdot}s^{-1}$), and ζ is the fraction of the $g_{c(\max)}$ at which the leaf is operating. For each species, g_{cb} was assumed to be 2 $mol{\cdot}m^{-2}{\cdot}s^{-1}$, a value found to be typical of field conditions with normal photosynthetic gas exchange (Collatz et al., 1991). g_m was assumed to be 0.079 $mol{\cdot}m^{-2}{\cdot}s^{-1}$ for *G. biloba* and 0.194 $mol{\cdot}m^{-2}{\cdot}s^{-1}$ for *Q. alba* and *Z. mioga*, based on Franks et al.'s (2014) values for *G. biloba* and *Q. robur*, respectively, which were back calculated from the calculated A_n values using the empirical relationship $g_m = 0.013 \times A_n$ (Epron et al., 1995; Evans and Von Caemmerer, 1996). $g_{c(\max)}$ was calculated using Equation 5, from Franks and Beerling (2009):

$$g_{c\,(\max)} = \frac{d}{v} \cdot SD \cdot a_{\max} / \left(l + \frac{\pi}{2} \sqrt{a_{\max}/\pi} \right) \quad (5)$$

where d is the diffusivity of CO_2 in air, v is the molar volume of air, l is stomatal pore depth estimated as equal to single guard cell width, and $a_{\max}$ is the maximum stomatal aperture, approximated as a fraction β of a circle with diameter equal to stomatal pore length (p), or $a_{\max} = \beta(\pi p^2/2)$. Values for d and v were calculated based on Equations 6 and 7 (Marrero and Mason, 1972; Royer et al., 2019), with Equation 7 based on ideal gas principles:

$$d = 1.87 \times 10^{-10} \left(\frac{T^{2.072}}{P} \right) \quad (6)$$

$$v = v_{STP} \left(\frac{T}{T_{STP}} \right) \left(\frac{P}{P_{STP}} \right) \quad (7)$$

where T is leaf temperature (K), P is atmospheric pressure (assumed to be 1 atm), T_{STP} is 273.15 K, P_{STP} is 1 atm, and v_{STP} is the molar volume of air at T_{STP} and P_{STP}

($0.022414\ m^3 \cdot mol^{-1}$). T used to calculate d and v was assumed to be 292.15 K, based on a mean temperature of 19°C for May through September in Ann Arbor, Michigan (PRISM Climate Group, 2020). *SD* was determined using measured values from each leaf sample calculated using Equation 2. Two methods were used to determine p, one using direct measurements of pore lengths for each sample and one using the approximate geometric relationship between guard cell length and pore length (p/L) described in the supplementary material of Franks et al. (2014). For the latter method, p/L was assumed to be 0.25 for *G. biloba*, 0.3 for *Q. alba*, and 0.6 for *Z. mioga* based on the plant type and stomata size (Franks et al., 2014). The Franks et al. (2014) approximate geometric relationships for β were used for both methods, using the measured and approximated pore length again based on plant type and stomata size (0.6 for *G. biloba*, 1.0 for *Q. alba*, and 0.4 for *Z. mioga*).

The theoretical relationship relating average c_i/c_a to carbon isotope discrimination from the air by a plant (Δ_{leaf}) described in Farquhar et al. (1982) was used to determine c_i/c_a:

$$c_i/c_a = \left[\frac{\Delta_{leaf} - a}{b - a}\right] \quad (8)$$

where a is the carbon isotope fractionation due to diffusion of CO_2 in air (4.4‰) (Farquhar et al., 1982), b is carbon isotope fractionation due to the carboxylation of ribulose bisphosphate (RuBP) (assumed to be 27–30‰) (Roeske and O'Leary, 1984), and Δ_{leaf} (‰) was determined using the relationship described in Farquhar and Richards (1984):

$$\Delta_{leaf} = \frac{\delta^{13}C_{air} - \delta^{13}C_{leaf}}{1 + \delta^{13}C_{leaf}/1000} \quad (9)$$

Each leaf was ground up and a 0.8-mg aliquot was combusted via Elemental Analyzer (Thermo Fisher Scientific, Bremen, Germany) and analyzed in a MAT 253 Gas Isotope Ratio Mass Spectrometer (Thermo Fisher Scientific) to determine its $\delta^{13}C_{leaf}$ values at the Stable Isotope and Organic Molecular Laboratory at the University of Connecticut. These values, and the $\delta^{13}C_{air}$ of −8.6675‰ at the time of collection (Keeling et al., 2001), were used to calculate Δ_{leaf}. The input spreadsheets for the Franks model calculations are available in Appendix S1.

RESULTS

The size, shape, arrangement, and overall appearance of the stomata and guard cells of the three species are each quite distinct (Figure 1). The results of the measurements of *SD*, *SI*, guard cell length, pore length, and guard cell pair width are shown in Figure 3 and Appendix S2. If there were no difference between any two methods, the results would theoretically follow a 1:1 line. Points that fall below the 1:1 line show that the method on the y-axis underestimated the value compared to the x-axis, while points above the line show that the method overestimated the value.

Fluorescence on cleared leaves

Compared to the other methods, clearing resulted in the smallest range in values for guard cell length, pore length, and guard cell pair width in all species (Figure 3, Table 1). However, this was not the case for *SD* and *SI*, and in *Z. mioga* clearing resulted in the largest range in these measurements (Table 1). In *G. biloba*, clearing showed markedly larger guard cell lengths and guard cell pair widths than all other methods, with no overlap in their ranges (Figure 3, Table 1). In *Q. alba*, clearing also resulted in larger guard cell lengths than the other three methods, although not to an extreme degree as there was some overlap in their ranges (Figure 3, Table 1).

Nail polish on fresh leaves

Compared to clearing, the polish method tended to underestimate *SD* in *G. biloba* (Table 1) and to overestimate *SD* in *Q. alba* (Figure 3, Table 1), but *SD* was not skewed in either direction in *Z. mioga* (Figure 3). Stomatal index was mostly overestimated by polish compared to clearing in *G. biloba* but was not consistently over- or underestimated in *Q. alba* and *Z. mioga* (Figure 3). In both *G. biloba* and *Q. alba*, the polish method underestimated guard cell length compared to clearing, while in *Z. mioga* this was mostly overestimated (Figure 3). The polish method tended to overestimate pore length in *Q. alba* and *Z. mioga* compared to clearing, while this was not shown in *G. biloba* (Figure 3). Guard cell pair width was mostly overestimated by the polish method compared to clearing for *Q. alba*, while it was underestimated for *G. biloba* and there was no consistent effect in *Z. mioga* (Figure 3). In *Z. mioga*, pore length measurements achieved using the polish method were larger and showed no overlap with clearing (Figure 3). In contrast, guard cell length and guard cell pair widths in *G. biloba* were smaller and showed no overlap with clearing measurements (Figure 3).

Dental putty on dried leaves

The putty on dried leaves method tended to underestimate *SD* and overestimate *SI* compared to clearing in *G. biloba*, although this was less uniform in *Q. alba* and *Z. mioga* (Figure 3). Putty on dried leaves also mostly underestimated guard cell length compared to clearing in all three species (Figure 3). Pore length was mostly overestimated by putty on dried leaves compared to clearing in *Q. alba* and *Z. mioga*, while no consistent effect was shown in *G. biloba* (Figure 3). Guard cell pair width was

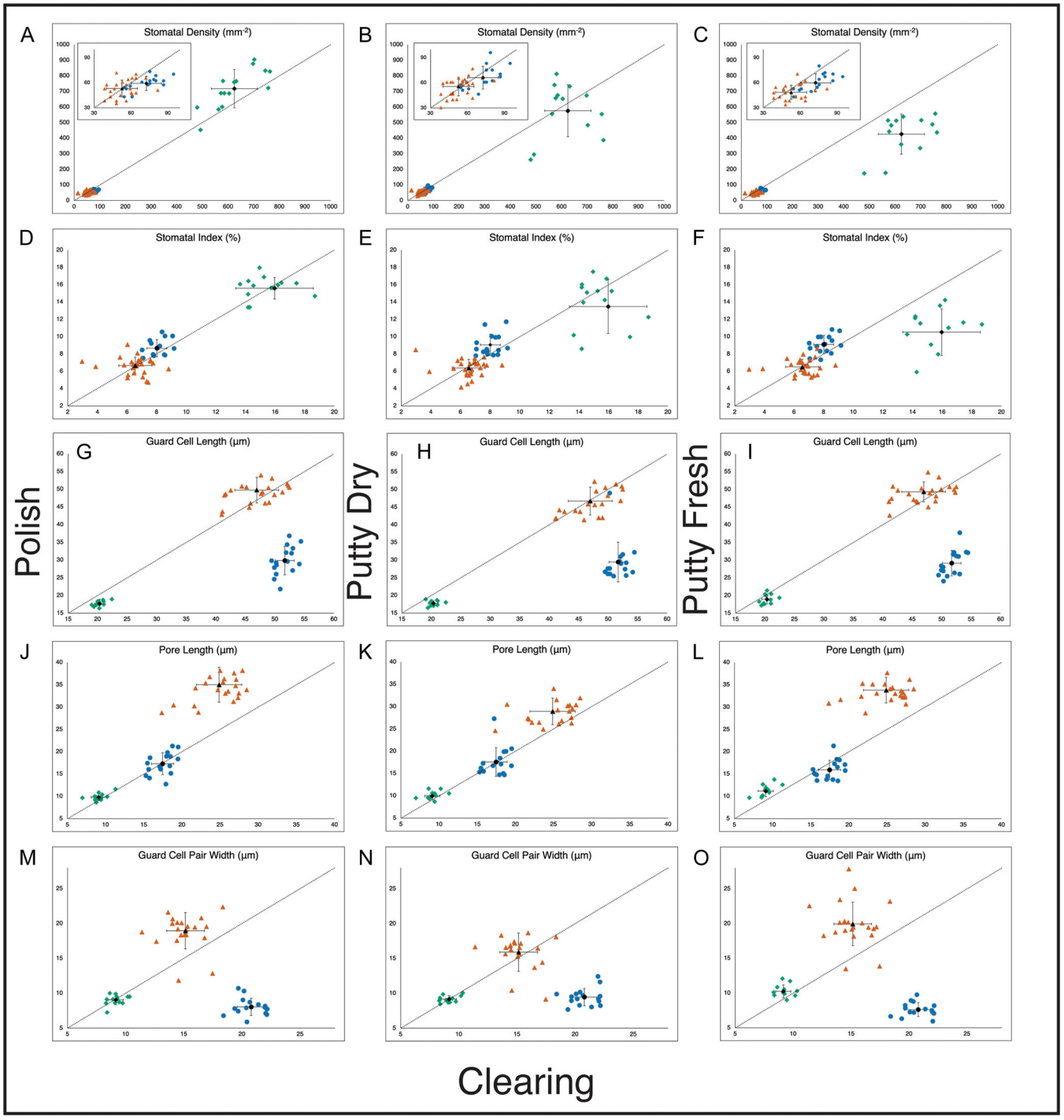

FIGURE 3 Comparison of stomatal traits between the three impression methods and the cleared leaf material. Each individual plot shows values for clearing on the *x*-axis, and either polish, putty on fresh leaves, or putty on dried leaves as labeled on the *y*-axis. The trait being compared is listed at the top of each plot. *Ginkgo biloba* is represented by blue circles, *Quercus alba* by green diamonds, and *Zingiber mioga* by orange triangles. Black symbols represent the mean for each species, with error bars showing one standard deviation. The dotted line shows the theoretical 1:1 relationship.

underestimated compared to clearing in *G. biloba*, while *Q. alba* and *Z. mioga* showed no consistent effects (Figure 3). There was no overlap between measured ranges of guard cell length and guard cell pair width using the putty on dried leaves and clearing methods for *G. biloba* (Figure 3, Table 1).

Dental putty on fresh leaves

The putty on fresh leaves method underestimated *SD* and overestimated *SI* compared to clearing in *G. biloba* (for *SD*: $t = 4.68$, $df = 92$, $P = 4.86 \times 10^{-6}$; for *SI*: $t = -3.88$, $df = 84$, $P = 2.09 \times 10^{-4}$), while in *Q. alba* both *SI* and *SD*

TABLE 1 Summary of trait measurements in the three focal taxa: *Ginkgo biloba*, *Quercus alba*, and *Zingiber mioga*.[a]

Species	Method	*SD* (No. of stomata mm^{-2})	*SI* (%)	Guard cell length (μm)	Pore length (μm)	Guard cell pair width (μm)
G. biloba	Clearing	72.51 (54.48–94.55) ± 12.38	8.01 (7.02–9.17) ± 0.67	51.68 (49.44–54.41) ± 1.58	17.46 (15.29–19.51) ± 1.45	20.79 (18.40–22.16) ± 1.20
G. biloba	Polish	59.39 (43.27–73.71) ± 8.47	8.67 (7.51–10.56) ± 0.99	29.84 (21.82–36.84) ± 4.01	17.31 (12.76–21.27) ± 2.46	8.04 (5.89–10.72) ± 1.23
G. biloba	Putty (dry)	66.20 (46.47–96.15) ± 13.58	9.06 (7.80–11.73) ± 1.24	29.44 (25.49–48.96) ± 5.63	17.59 (14.70–27.30) ± 3.21	9.46 (7.68–12.44) ± 1.25
G. biloba	Putty (fresh)	59.99 (43.27–80.12) ± 10.90	9.10 (7.34–10.84) ± 1.04	29.15 (24.08–37.76) ± 3.60	15.93 (13.49–21.34) ± 2.15	7.63 (5.96–9.77) ± 0.99
Q. alba	Clearing	624.65 (479.14–762.78) ± 90.19	15.96 (13.63–24.00) ± 2.62	20.32 (19.00–22.42) ± 0.87	9.10 (6.96–11.30) ± 1.00	9.15 (8.31–10.33) ± 0.65
Q. alba	Polish	717.59 (453.50–905.40) ± 122.83	15.59 (13.40–17.97) ± 1.23	17.67 (16.40–18.94) ± 0.73	9.80 (8.65–11.62) ± 0.73	9.04 (7.25–10.01) ± 0.70
Q. alba	Putty (dry)	576.09 (262.81–812.46) ± 166.70	13.48 (7.89–17.51) ± 3.13	17.75 (16.48–18.93) ± 0.70	9.96 (8.73–11.65) ± 0.88	9.17 (8.47–10.06) ± 0.48
Q. alba	Putty (fresh)	426.14 (174.67–557.66) ± 128.44	10.52 (5.51–14.24) ± 2.70	18.93 (17.19–21.42) ± 1.33	11.19 (9.72–13.79) ± 1.28	10.25 (8.88–12.10) ± 0.93
Z. mioga	Clearing	52.62 (14.42–81.72) ± 12.58	6.55 (2.96–8.80) ± 1.12	46.94 (41.01–52.45) ± 3.72	24.87 (17.36–28.48) ± 2.97	15.14 (11.40–18.35) ± 1.63
Z. mioga	Polish	53.23 (35.25–72.11) ± 9.94	6.66 (4.73–9.09) ± 0.97	49.77 (42.85–57.40) ± 3.61	35.01 (28.73–43.98) ± 3.92	18.97 (11.85–22.64) ± 2.61
Z. mioga	Putty (dry)	55.57 (30.45–76.92) ± 11.03	6.40 (4.17–8.49) ± 0.97	46.72 (41.38–56.59) ± 3.95	28.92 (23.14–35.53) ± 2.98	15.91 (8.98–19.37) ± 2.74
Z. mioga	Putty (fresh)	48.70 (33.65–70.51) ± 8.42	6.51 (5.2–8.64) ± 0.88	49.32 (42.66–54.82) ± 2.82	33.80 (28.68–40.56) ± 2.87	19.95 (13.13–27.85) ± 3.13

[a]Mean values are presented, with the range in parentheses and one standard deviation following the '±' symbol for stomatal density (*SD*), stomatal index (*SI*), guard cell length, pore length, and guard cell pair width for the four preparation methods.

were underestimated compared to clearing (for *SD*: $t = 5.96$, $df = 56$, $P = 8.74 \times 10^{-8}$; for *SI*: $t = 5.66$, $df = 78$, $P = 1.22 \times 10^{-7}$; Figure 3). The results for *Z. mioga* showed no significant difference between methods for *SD* and *SI* (Figure 3, Table 1). Guard cell length, pore length, and guard cell pair width were all underestimated using putty on fresh leaves compared to clearing in *G. biloba* (Figure 3). Guard cell length was underestimated using putty on fresh leaves compared to clearing in *Q. alba*, while pore length and guard cell pair width were overestimated (Figure 3). Pore length and guard cell pair width were overestimated using putty on fresh leaves compared to clearing in *Z. mioga*, while guard cell length did not show a similar effect (Figure 3).

Calculated c_a

The results of the c_a calculations tended to overestimate the c_a value most of the time (Figure 4, Appendix S2). The mean

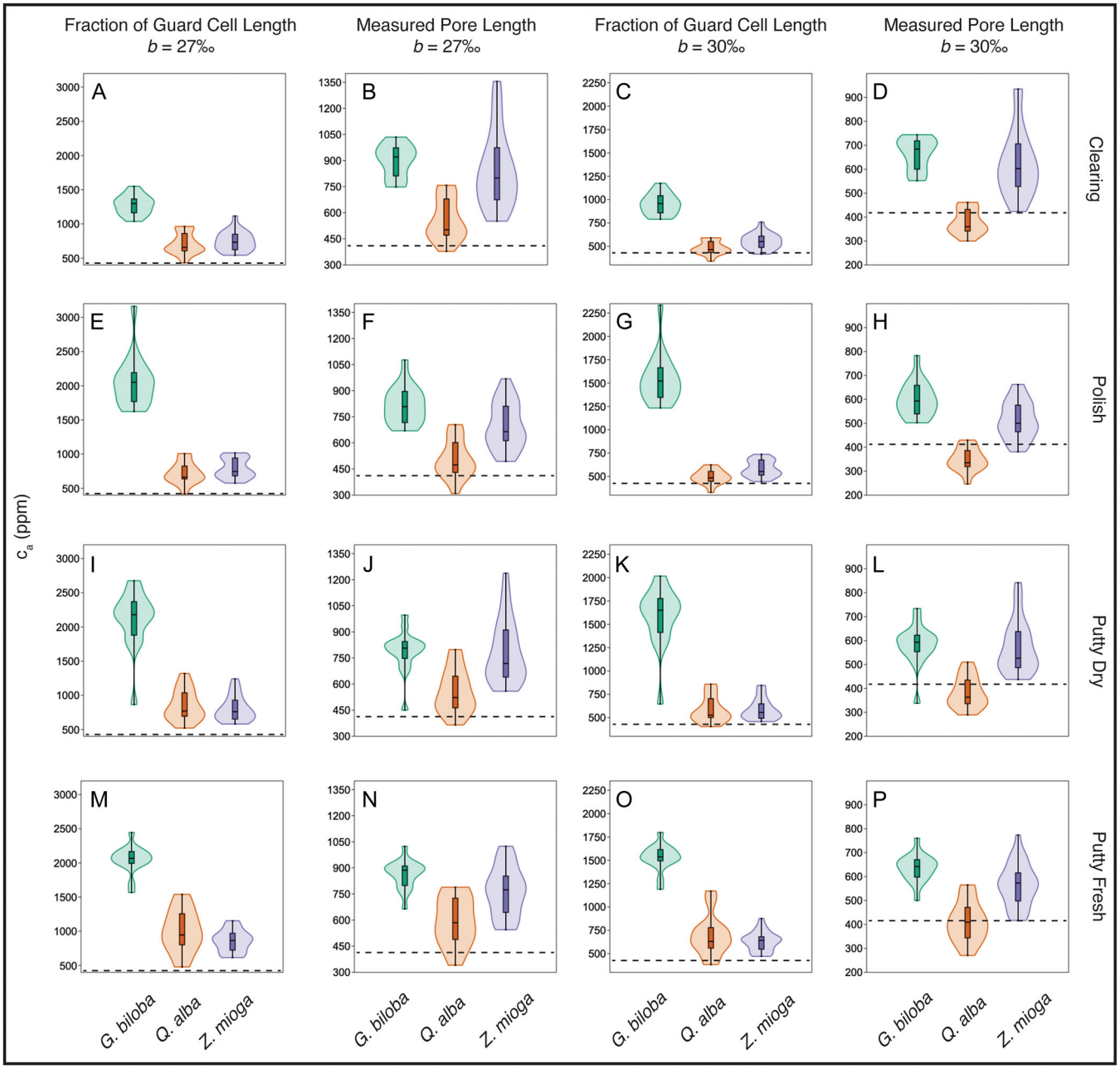

FIGURE 4 Comparison of calculated c_a values using different parameters. (A–D) Cleared leaves under fluorescence, (E–H) polish, (I–L) putty on dry leaves, (M–P) putty on fresh leaves. Values were calculated with either measured (B, D, F, H, J, L, N, P) or estimated (A, C, E, G, I, K, M, O) pore length, and *b* values of either 27‰ (A, B, E, F, I, J, M, N) or 30‰ (C, D, G, H, K, L, O, P). Box-and-whisker plots show the data range, median, and 25th and 7th quartiles. Shaded area is a kernel density plot. The dashed line represents the actual c_a value of 416.45 ppm.

c_a estimate for each species using each method was always higher than the true value, except for in *Q. alba* when $b = 30‰$ and measured pore length was used (Figure 4). Overall, c_a was most accurately predicted in *Q. alba*, where the true value was within the range of calculated values in every case when pore length was measured, or when $b = 30‰$ (Figure 4, columns B–D; Table 2). All *G. biloba* estimates were higher than the true c_a except for using putty on dried leaves when $b = 30‰$ and measured pore length was used (Figure 4L, Table 2). *Zingiber mioga* also completely overestimated c_a in every case except when using the clearing method with a fraction of guard cell length and $b = 30‰$ and when using putty on fresh leaves with pore length and $b = 30‰$ (Figure 4C, P; Table 2). In every case with a b value of 27‰, all estimated c_a values for *G. biloba* and *Z. mioga*, as well as the mean estimate for all three species, were higher than the true value of 416.45 ppm (Figure 4A, B, E, F, I, J, M, N; Table 2).

When measured pore length was used, the mean c_a estimates for *Q. alba* using each method were not significantly different from one another (for $b = 27‰$: $F_{3,51} = 1.11$, $P = 0.35$; for $b = 30‰$: $F_{3,51} = 2.15$, $P = 0.11$), regardless of whether a b value of 27‰ or 30‰ was used, and while there were significant differences between methods for *G. biloba* (for $b = 27‰$: $F_{3,60} = 3.67$, $P = 0.02$; for $b = 30‰$: $F_{3,60} = 4.31$, $P = 0.01$) and *Z. mioga* (for $b = 27‰$: $F_{3,99} = 3.04$, $P = 0.03$; for $b = 30‰$: $F_{3,99} = 4.54$, $P = 0.01$), their mean estimates were still within one standard deviation of one another (Table 2). When guard cell length was used, clearing showed significantly lower mean c_a estimates than the other three methods for *G. biloba* ($F_{3,60} = 26.6$, $P = 4.57 \times 10^{-11}$) and *Q. alba* ($F_{3,51} = 5.06$, $P = 0.004$) (Table 2), but *Z. mioga* showed no significant difference in mean estimates when $b = 27‰$ ($F_{3,99} = 1.98$, $P = 0.12$) (Table 2). For each species and each method, the mean c_a estimate was closest to the true value when measured pore length was used and $b = 30‰$ (Table 2), except in the case of using clearing with guard cell length and $b = 30‰$ for *Z. mioga* (Table 2).

Difference between counters

Depending on the measurement being made and the species analyzed, the differences between the values obtained by each of the three counters ranged from very small to significantly different. Mean *SD* measurements were consistent between counters for *Z. mioga* (clearing: $F_{2,78} = 0.50$, $P = 0.61$; putty on dried leaves: $F_{2,81} = 1.47$, $P = 0.24$), for *G. biloba* using the clearing method ($F_{2,45} = 2.01$, $P = 0.15$), and for *Q. alba* using putty on dried leaves ($F_{2,41} = 2.49$, $P = 0.10$) (Figure 5, Tables 3–5, Appendix S2). Mean *SI* measurements for *G. biloba* and *Z. mioga* were also fairly consistent between all counters, although for *Q. alba* one counter recorded higher values than the others (Figure 5, Tables 3–5). Guard cell length is very well constrained between the three counters in *G. biloba* (clearing: $F_{2,45} = 1.54$, $P = 0.22$; putty on dried leaves: $F_{2,45} = 2.28$, $P = 0.11$), but less so in *Z. mioga* while still showing a consistency in measurement (clearing: $F_{2,72} = 1.95$, $P = 0.15$; putty on dried leaves: $F_{2,79} = 1.14$, $P = 0.32$) (Figure 5; Tables 3, 5). However, in *Q. alba*, one counter again shows distinctly different measurements than the other two (clearing: $F_{2,40} = 23.4$, $P = 1.85 \times 10^{-7}$; putty on dried leaves: $F_{2,42} = 48.1$, $P = 1.35 \times 10^{-11}$) (Figure 5, Table 4). While the data as a whole shows some overlap, mean pore length in all three species shows some degree of distinction between counters, although one counter obtained more significant differences for *Z. mioga* (clearing: $F_{2,72} = 223$, $P = 1.34 \times 10^{-31}$; putty on dried leaves: $F_{2,79} = 29.3$, $P = 3.03 \times 10^{-10}$) (Figure 5, Tables 3–5). Guard cell pair width showed the largest differences between counters, with almost no overlap among the results from each counter for each of the three species (Figure 5, Tables 3–5).

DISCUSSION

Differences between methods

Clearing is likely the most accurate of the four methods for examining stomatal characteristics because it uses the actual leaf rather than an impression of the cuticle. Studying cleared leaves under a fluorescence light microscope allows for cell layers beyond the outermost cuticle to be examined at different magnifications and also allows for greater visibility into the entire structure of stomata beyond this outermost cell layer. In contrast, the other three methods record an impression of only the outermost layer of the leaf cuticle, and in the case of the putty molds, an impression of an impression. Smaller guard cell lengths were measured from each method compared to clearing in *G. biloba* and *Q. alba*, as were guard cell pair widths in *G. biloba*. In contrast, pore length measurements were less sensitive to each method in either species. Given that guard cell length and guard cell pair width are both measurements of the edges of stomata and pore length is not, the impressions are likely not capturing complete stomatal anatomy and are thus more sensitive to methodological differences. *Ginkgo biloba* leaves have sunken stomata and overarching papillae (Gray et al., 2020), which would explain the inability of impressions to represent complete stomata. While *Q. alba* leaves do not have sunken stomata, their stomata are much smaller overall and likely more sensitive to differences in method, explaining the slightly smaller values for guard cell length. This suggests that clearing is a more accurate method of examining stomatal traits in these species, as it captures a more complete view of the stomata regardless of stomatal morphology. Use of scanning electron microscopy of treated leaf cuticles, as done by Barclay and Wing (2016), may provide even more accurate stomatal measurements than the use of fluorescence light microscopy, as the three-dimensional stomatal morphology is better imaged, and further insights may be made by comparing the two methods (Matthaeus et al., 2020).

TABLE 2 Summary of calculated c_a for four preparation methods using different input parameter values.[a]

Species	Method	GCL, b = 27‰	PL, b = 27‰	GCL, b = 30‰	PL, b = 30‰
G. biloba	Clearing	1278.60 (1036.90–1549.68) ± 143.21	899.84 (748.03–1034.54) ± 93.97	951.95 (789.16–1174.55) ± 111.56	665.30 (552.02–744.06) ± 65.57
G. biloba	Polish	2061.48 (1622.14–3161.51) ± 376.67	816.47 (669.35–1076.51) ± 107.07	1543.05 (1232.49–2334.75) ± 266.76	600.60 (502.27–783.02) ± 72.95
G. biloba	Putty (dry)	2115.34 (864.46–2674.93) ± 425.29	789.78 (450.78–996.31) ± 119.68	1582.69 (645.70–2015.69) ± 321.31	581.67 (338.13–733.85) ± 86.62
G. biloba	Putty (fresh)	2048.54 (1566.56–2444.12) ± 201.07	862.66 (664.38–1023.79) ± 83.02	1527.97 (1189.73–1797.88) ± 141.86	635.37 (500.24–760.40) ± 57.75
Q. alba	Clearing	710.52 (432.40–963.75) ± 161.13	559.82 (378.03–757.43) ± 122.07	481.54 (339.95–590.20) ± 73.37	380.63 (299.89–461.47) ± 52.77
Q. alba	Polish	722.65 (418.06–1007.97) ± 159.27	506.49 (309.39–704.90) ± 110.34	495.86 (329.30–623.93) ± 75.38	349.13 (246.40–429.94) ± 49.07
Q. alba	Putty (dry)	851.03 (520.22–1319.61) ± 230.27	557.17 (365.39–798.52) ± 127.12	585.86 (404.27–858.85) ± 141.99	383.95 (289.50–509.98) ± 65.34
Q. alba	Putty (fresh)	1004.77 (479.02–1540.01) ± 313.95	590.95 (340.94–788.99) ± 139.66	699.23 (382.81–1170.29) ± 221.73	410.72 (270.53–565.28) ± 86.21
Z. mioga	Clearing	746.46 (542.40–1116.24) ± 144.37	843.52 (551.78–1354.94) ± 217.57	552.73 (415.91–758.75) ± 84.72	623.04 (423.21–935.05) ± 137.54
Z. mioga	Polish	791.39 (574.89–1017.65) ± 145.76	699.67 (493.55–968.13) ± 132.36	581.58 (444.41–736.36) ± 87.60	513.53 (380.90–662.17) ± 78.57
Z. mioga	Putty (dry)	801.19 (579.80–1241.08) ± 185.53	782.83 (559.07–1237.46) ± 179.89	587.35 (457.23–845.64) ± 113.69	573.30 (437.28–842.08) ± 109.21
Z. mioga	Putty (fresh)	855.98 (615.42–1153.87) ± 160.68	764.79 (544.76–1024.72) ± 141.01	631.71 (470.82–876.96) ± 103.38	563.92 (416.80–773.78) ± 89.27

Note: GCL = guard cell length; PL = pore length.

[a]Mean values are presented, with the range in parentheses and one standard deviation following the '±' symbol.

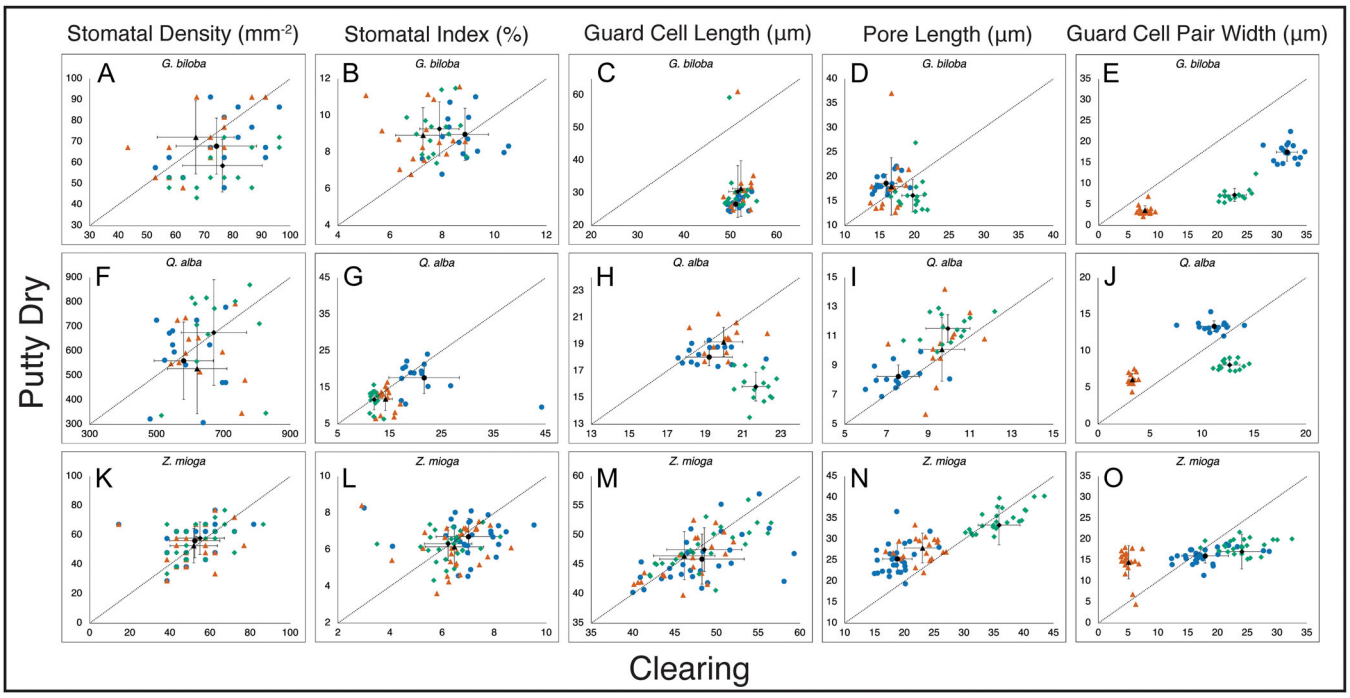

FIGURE 5 Differences between three counters for measured trait values from putty on dried leaves and cleared leaves under fluorescence. (A, F, K) Stomatal density, (B, G, L) stomatal index, (C, H, M) guard cell length, (D, I, N) pore length, (E, J, O) guard cell pair width. The measurements of counter 1 are represented by blue circles, counter 2 by green diamonds, and counter 3 by orange triangles. Black symbols represent the mean for each species, with error bars showing one standard deviation. The dotted line shows the theoretical 1:1 relationship.

Surprisingly, using dried rather than fresh leaves to measure stomata did not lead to smaller stomatal measurements as was expected due to potential shrinking from desiccation. The only significantly smaller measurements on dried leaves were of guard cell length and guard cell pair width in *G. biloba* and of pore length in *Q. alba*; however, these values were similarly lower for the other impression methods on fresh leaves. This means either that the stomata undergo similar shrinkage effects from being pressed and dried as from being removed from the plant or that this is a result of the impressions themselves. While *Z. mioga* also appeared to show slightly smaller guard cell length in impressions of dried leaves than fresh leaves, pore length and guard cell pair width were actually larger for all three impression methods. This again does not support a shrinking of stomata due to desiccation.

Effects on c_a calculations

While individual stomatal measurements could be quite sensitive to differences between the methods, c_a was less sensitive to these differences, except for measured pore length. True c_a could only be calculated within the range of values using guard cell length on *Q. alba* when $b = 30‰$ (Figure 4). This shows that using measured pore length, rather than estimating it as a fraction of guard cell length, is the best method for calculating c_a, and researchers should strive to find fossils with stomatal apertures preserved for use in the Franks model.

The results also demonstrate the importance of b in the calculation of c_a, as a three per mil difference in this value led to significantly different ranges in calculated c_a values for each method and species (Figure 4, Table 2). The degree to which carboxylation of RuBP fractionates ^{13}C in each species should be directly measured in extant species or the most closely related extant species for the most accurate results, rather than relying on a single constant value. Another approach that can resolve this is using a best-fit model to determine an optimal b value for a species, as done in Scher et al. (2022). Even within closely related lineages (e.g., gymnosperms), Δ_{leaf} is highly variable beyond the 18–22‰ that is typical for C_3 plants (Sheldon et al., 2020), and one way that quantity can vary is through differences in isotope fractionation from RuBP. The results suggest each of the three taxa are expressing RuBisCO closer to a b value of 30‰, and that this value can be assumed for modern c_a levels. Furthermore, incorporating other processes such as fractionation due to photorespiration and the CO_2 compensation point in the absence of dark respiration may lead to higher c_a estimates closer to the true value (Royer et al., 2019). Similarly, better refining values for A_n, g_m, β, and T based on these specific taxa may lead to more accurate c_a estimates, and further study of these for each taxa is recommended.

The results of these calculations suggest that using original material, as in the clearing method, or using cuticle impressions, as in the other three methods, does produce significantly different c_a estimates in some cases using the

TABLE 3 Summary of counter-specific measurements for *Ginkgo biloba*.[a]

Counter	Method	*SD* (No. of stomata mm^{-2})	*SI* (%)	Guard cell length (μm)	Pore length (μm)	Guard cell pair width (μm)
1	Clearing	74.21 (52.88–96.15) ± 14.04	8.88 (7.24–10.55) ± 0.90	51.16 (49.00–54.59) ± 1.64	15.94 (13.96–19.38) ± 1.54	31.69 (27.68–34.68) ± 1.75
2	Clearing	67.00 (43.27–91.34) ± 13.42	7.27 (5.08–8.88) ± 1.05	52.28 (48.50–54.95) ± 1.82	16.69 (13.66–19.18) ± 1.69	7.81 (6.43–9.53) ± 0.90
3	Clearing	76.32 (57.69–100.96) ± 13.92	7.90 (6.64–9.52) ± 0.75	51.61 (48.86–55.67) ± 1.96	19.77 (16.61–21.89) ± 1.57	22.87 (20.23–26.45) ± 1.98
1	Putty (dry)	67.90 (48.07–91.34) ± 13.35	8.97 (6.80–12.13) ± 1.43	26.52 (24.28–30.42) ± 1.79	18.62 (16.26–22.16) ± 1.85	17.52 (14.60–22.46) ± 2.18
2	Putty (dry)	72.11 (48.07–110.57) ± 17.47	8.92 (6.79–11.57) ± 1.51	31.37 (24.75–61.10) ± 8.51	18.00 (12.67–37.05) ± 5.88	3.60 (2.13–6.96) ± 1.10
3	Putty (dry)	58.59 (43.27–91.34) ± 12.56	9.27 (7.40–12.40) ± 1.48	30.42 (26.25–59.26) ± 7.93	16.14 (12.87–26.94) ± 3.32	7.28 (5.44–12.36) ± 1.56

[a]Mean values are presented, with the range in parentheses and one standard deviation following the '±' symbol for stomatal density (*SD*), stomatal index (*SI*), guard cell length, pore length, and guard cell pair width for cleared leaves under fluorescence and putty on dried leaves.

TABLE 4 Summary of counter-specific measurements for *Quercus alba*.[a]

Counter	Method	*SD* (No. of stomata mm^{-2})	*SI* (%)	Guard cell length (μm)	Pore length (μm)	Guard cell pair width (μm)
1	Clearing	581.06 (408.63–706.69) ± 88.81	21.65 (17.23–44.23) ± 6.76	19.21 (17.58–22.22) ± 1.23	7.56 (5.99–10.02) ± 1.02	11.16 (7.55–14.06) ± 1.53
2	Clearing	621.44 (480.74–764.38) ± 88.80	14.22 (12.32–17.05) ± 1.34	19.98 (18.17–22.28) ± 1.01	9.66 (7.08–11.70) ± 1.09	3.29 (2.89–3.89) ± 0.30
3	Clearing	671.44 (514.40–826.88) ± 97.63	12.02 (11.17–13.89) ± 0.71	21.67 (20.53–22.77) ± 0.72	9.94 (7.81–12.81) ± 1.06	12.65 (11.06–14.53) ± 1.00
1	Putty (dry)	559.91 (288.45–778.80) ± 158.25	17.67 (9.66–24.14) ± 4.36	18.25 (17.34–19.31) ± 0.66	8.26 (6.90–9.96) ± 0.79	13.37 (12.04–15.38) ± 0.73
2	Putty (dry)	527.54 (221.14–793.23) ± 184.24	11.87 (6.55–16.48) ± 3.18	19.18 (17.69–21.30) ± 1.10	10.10 (5.69–14.22) ± 2.16	6.06 (4.42–7.57) ± 0.83
3	Putty (dry)	675.44 (278.83–975.91) ± 215.74	11.69 (6.37–15.74) ± 2.77	15.83 (13.53–17.44) ± 1.08	11.53 (9.95–12.93) ± 0.95	8.09 (7.26–9.12) ± 0.64

[a]Mean values are presented, with the range in parentheses and one standard deviation following the '±' symbol for stomatal density (*SD*), stomatal index (*SI*), guard cell length, pore length, and guard cell pair width for cleared leaves under fluorescence and putty on dried leaves.

TABLE 5 Summary of counter-specific measurements for *Zingiber mioga*.[a]

Counter	Method	*SD* (No. of stomata mm^{-2})	*SI* (%)	Guard cell length (μm)	Pore length (μm)	Guard cell pair width (μm)
1	Clearing	52.37 (14.42–81.73) ± 12.50	7.01 (3.01–9.52) ± 1.25	48.26 (39.98–59.29) ± 5.06	18.83 (14.99–25.80) ± 2.47	17.92 (12.27–28.67) ± 3.93
2	Clearing	51.85 (14.42–76.92) ± 11.80	6.47 (2.91–8.65) ± 1.12	46.14 (40.11–52.02) ± 3.68	23.03 (16.85–29.07) ± 3.02	5.08 (3.84–7.38) ± 1.02
3	Clearing	55.00 (38.46–86.53) ± 12.18	6.23 (3.50–8.24) ± 0.91	48.53 (41.99–56.52) ± 4.50	35.86 (30.23–43.47) ± 30.23	24.07 (17.14–32.48) ± 3.51
1	Putty (dry)	56.14 (28.84–76.92) ± 11.63	6.71 (4.55–8.28) ± 1.00	45.91 (40.23–57.00) ± 4.27	25.33 (19.39–36.63) ± 3.66	16.04 (11.42–18.84) ± 1.70
2	Putty (dry)	52.71 (28.84–76.92) ± 11.66	6.16 (3.61–8.41) ± 1.15	46.47 (39.78–56.75) ± 4.09	27.90 (18.30–34.53) ± 3.54	14.51 (3.25–19.39) ± 3.96
3	Putty (dry)	57.86 (33.65–76.92) ± 11.06	6.32 (4.33–8.78) ± 0.91	47.51 (40.59–56.02) ± 3.73	33.37 (21.07–40.29) ± 4.70	17.07 (5.87–21.73) ± 4.16

[a]Mean values are presented, with the range in parentheses and one standard deviation following the '±' symbol for stomatal density (*SD*), stomatal index (*SI*), guard cell length, pore length, and guard cell pair width for cleared leaves under fluorescence and putty on dried leaves.

Franks model. Looking specifically at the estimates using measured pore length and a *b* value of 30‰, there is no significant difference between methods for *Q. alba*, and while there is a significant difference between methods for *G. biloba* and *Z. mioga*, the mean estimates are all within one standard deviation of one another. This is contrary to the results of Stein et al. (2024), which showed that significant differences between guard cell width measurements in cleared leaves and impressions produced significantly different c_a estimates. However, there may be taxon-specific effects on stomatal measurements based on different methods, as Stein et al. (2024) used leaves from *Populus tremuloides* Michx. and various *Thuja* L. species, which are not closely related to any of the taxa investigated in this study. The results also reinforce the importance of using as many leaves as possible when estimating c_a using the Franks model, as leaves growing under the same atmospheric conditions generated ranges sometimes in excess of 1000 ppm using estimated pore length (*G. biloba* using polish or putty on dry leaves with either *b* value) and in excess of 800 ppm using measured pore length (*Z. mioga* using clearing when $b = 27‰$) (Table 2).

Ginkgo L. is widely used as a paleo-CO_2 barometer because of the similarity of modern *G. biloba* to the fossil *G. adiantoides* (Unger) Heer (Tralau, 1968; Royer et al., 2003; Barclay and Wing, 2016). Given that it is so widely used, it is especially important to understand how measurements of *Ginkgo*'s stomata might be affected by differences in cuticle preparation method, not just between impressions versus original material but also between clearing/staining methods. The tendency for calculations to overestimate the actual c_a using *G. biloba* is consistent with previous applications of the Franks model (Franks et al., 2014; Royer et al., 2019). Of the 16 combinations of cuticle preparation method, means of measuring pore length, and *b* value, only one had the true c_a within the range of its calculations, versus 13/16 for *Q. alba* (Figure 4). This highlights the need to standardize calibration of the Franks model for paleo-CO_2 barometry that is probably usually overestimating c_a, as Scher et al. (2022) did for *G. biloba*.

The largely inaccurate c_a values produced in this study highlight some of the shortcomings of the Franks model. Even with careful attention to detail, the model can still produce inaccurate reconstructions of even ambient c_a. This is to some extent accounted for when a *b* value of 30‰ is used, but even then, estimates can be far greater than actual ambient c_a. While previous studies have shown accurate reconstructions of ambient c_a using the Franks model (Franks et al., 2014; Royer et al., 2019; Steinthorsdottir et al., 2022), our results show that there is also potential for the model to produce overestimates (or, rarely, underestimates) under these conditions and also highlight the variability between species, suggesting a need for more taxon-specific calibrations. The model should continue to be tested on modern taxa growing at ambient atmospheric CO_2 concentrations and refined to ensure paleoclimatic reconstructions are producing accurate results.

Differences between counters

It is very important that those making measurements of stomata are familiar with stomatal morphology and the variation it can have across taxa. Guard cell pair width measurements from each counter were entirely distinct from each other, with no overlap in *G. biloba* or *Z. mioga*. One counter consistently tended to under-measure guard cell pair width in each of the three species in every method. Similarly, one counter mostly over-measured pore length for each species compared to the others. This stresses the importance of being familiar with stomatal anatomy and using standardized measurement procedures when analyzing stomata, but also suggests that doing replicated counts by different individuals and averaging the results will likely do a better job of capturing variation than relying on a single counter. While we tried to standardize the procedure for cell counting and measurement between each person, people still interpreted the edges of guard cells and which cells to count or not count around the edges of the image differently. These two areas of inconsistency specifically should be addressed clearly when stomatal analysis is done by more than one person for a given dataset, as well as to ensure inter-lab data compatibility. For example, following the procedures laid out by Poole and Kürschner (1999) should help standardize procedure between counters and constrain human error. Workshops or other opportunities for multiple people and multiple labs/groups to be trained together might also offer good venues for discussing such nuances to the procedures and promote consistency.

Measurements of *Z. mioga* were the most consistent between counters, while those of *Q. alba* were clearly the least consistent. The consistency of *Z. mioga* measurements is likely due to its larger, non-sunken stomata flanked by pairs of subsidiary cells and hexagonal epidermal cells arranged in a fairly uniform, brick-like manner without subsidiary cells (Figure 1). In contrast, *Q. alba* has much smaller stomata and epidermal cells arranged in a much less uniform manner (Figure 1). Additionally, the leaves of *Q. alba* have denser, reticulate venation, making it difficult to avoid leaf veins in images of the cuticle at the level of magnification used. Reexamining *Q. alba* cuticles at a higher magnification may lead to more consistent results across counters.

Concluding remarks

It is important to consider the method of cuticle preparation when reconstructing [CO_2] using stomatal parameters, as different methods of cuticle preparation yield significantly different stomatal measurements. While these differences are less pronounced on the actual c_a calculations than on the measurements themselves, at higher [CO_2] levels, the effects could be more pronounced. Similarly, it is important to recognize how the effects of each method differ between taxa, as the most accurate *G. biloba* and *Z. mioga* calculations appeared to overestimate c_a, while those of *Q. alba* underestimated c_a. Our results suggest that when pore length is directly measured, any of the four methods tested can be used for c_a reconstructions, although those using the Franks model to make such reconstructions may prefer to use original material when possible, based on studies of other taxa. When pore length cannot be measured and must be estimated using guard cell length, how it will affect c_a calculations should be considered and, if possible, quantified. Our results also indicated that for the three species investigated, the operating b value is closer to 30‰ than to 27‰. Further study into species-specific ^{13}C fractionation due to carboxylation of RuBP may also help produce more accurate c_a calculations using stomatal measurements. Additionally, attention should be paid to how measurements are being made when more than one person is involved in making stomatal measurements and procedure should be strictly consistent across any people making measurements.

AUTHOR CONTRIBUTIONS

S.Y.S. and N.D.S. conceived the research and designed the study; M.D.M. prepared the leaf cuticles, measured stomata, and prepared leaf tissue samples for isotope analysis; M.T.H. performed isotope analysis. M.D.M., S.Y.S., and N.D.S. analyzed the data and wrote the manuscript. S.Y.S. and M.D.M. acquired the funding. All authors approved the final version of the manuscript.

ACKNOWLEDGMENTS

The authors thank Kelly Martin, Kate Morrison, and Katherine Harpenau (University of Michigan) for assistance with data collection, as well as two anonymous reviewers and the editors for their helpful feedback to improve the paper. This work was financed by the University of Michigan Department of Earth and Environmental Sciences Scott Turner Award (2021, 2022) and by the National Science Foundation (EAR–1949151 to S.Y.S.).

DATA AVAILABILITY STATEMENT

All data connected to the study are available in the manuscript and Supporting Information.

ORCID

Michael D. Machesky http://orcid.org/0009-0003-3959-4248
Nathan D. Sheldon http://orcid.org/0000-0003-3371-0036
Michael T. Hren http://orcid.org/0000-0002-2866-8892
Selena Y. Smith http://orcid.org/0000-0002-5923-0404

REFERENCES

Barclay, R. S., and S. L. Wing. 2016. Improving the *Ginkgo* CO_2 barometer: Implications for the early Cenozoic atmosphere. *Earth and Planetary Science Letters* 439: 158–171.

Collatz, G. J., J. T. Ball, C. Grivet, and J. A. Berry. 1991. Physiological and environmental regulation of stomatal conductance, photosynthesis and transpiration: A model that includes a laminar boundary layer. *Agricultural and Forest Meteorology* 54: 107–136.

Epron, D., D. Godard, G. Cornic, and B. Genty. 1995. Limitation of net CO_2 assimilation rate by internal resistances to CO_2 transfer in the leaves of two tree species (*Fagus sylvatica* L. and *Castanea sativa* Mill.). *Plant, Cell & Environment* 18: 43–51.

Evans, J. R., and S. Von Caemmerer. 1996. Carbon dioxide diffusion inside leaves. *Plant Physiology* 110: 339–346.

Farquhar, G. D., and T. D. Sharkey. 1982. Stomatal conductance and photosynthesis. *Annual Review of Plant Physiology* 33: 317–345.

Farquhar, G., and R. Richards. 1984. Isotopic composition of plant carbon correlates with water-use efficiency of wheat genotypes. *Functional Plant Biology* 11: 539.

Farquhar, G. D., M. H. O'Leary, and J. A. Berry. 1982. On the relationship between carbon isotope discrimination and the intercellular carbon dioxide concentration in leaves. *Functional Plant Biology* 9: 121–137.

Franks, P. J., and D. J. Beerling. 2009. Maximum leaf conductance driven by CO_2 effects on stomatal size and density over geologic time. *Proceedings of the National Academy of Sciences, USA* 106: 10343–10347.

Franks, P. J., D. L. Royer, D. J. Beerling, P. K. Van de Water, D. J. Cantrill, M. M. Barbour, and J. A. Berry. 2014. New constraints on atmospheric CO_2 concentration for the Phanerozoic. *Geophysical Research Letters* 41: 4685–4694.

Gray, A., L. Liu, and M. Facette. 2020. Flanking support: How subsidiary cells contribute to stomatal form and function. *Frontiers in Plant Science* 11: e881.

Hilu, K. W., and J. L. Randall. 1984. Convenient method for studying grass leaf epidermis. *Taxon* 33: 413–415.

Keeling, C. D., S. C. Piper, R. B. Bacastow, M. Wahlen, T. P. Whorf, M. Heimann, and H. A. Meijer. 2001. Exchanges of atmospheric CO_2 and $^{13}CO_2$ with the terrestrial biosphere and oceans from 1978 to 2000. Global aspects, SIO Reference Series, No. 01-06, Scripps Institute of Oceanography, San Diego, California, USA.

Konrad, W., D. L. Royer, P. J. Franks, and A. Roth-Nebelsick. 2021. Quantitative critique of leaf-based paleo-CO_2 proxies: Consequences for their reliability and applicability. *Geological Journal* 56: 886–902.

Kowalczyk, J. B., D. L. Royer, I. M. Miller, C. W. Anderson, D. J. Beerling, P. J. Franks, M. Grein, et al. 2018. Multiple proxy estimates of atmospheric CO_2 from an early Paleocene rainforest. *Paleoceanography and Palaeoclimatology* 33: 1427–1438.

Marrero, T. R., and E. A. Mason. 1972. Gaseous diffusion coefficients. *Journal of Physical and Chemical Reference Data* 1: 3–118.

Matthaeus, W. J., J. Schmidt, J. D. White, and B. Zechmann. 2020. Novel perspectives on stomatal impressions: Rapid and non-invasive surface characterization of plant leaves by scanning electron microscopy. *PLoS ONE* 15: e0238589.

McElwain, J. C. 2018. Paleobotany and global change: Important lessons for species to biomes from vegetation responses to past global change. *Annual Review of Plant Biology* 69: 761–787.

McElwain, J. C., and W. G. Chaloner. 1995. Stomatal density and index of fossil plants track atmospheric carbon dioxide in the Palaeozoic. *Annals of Botany* 76: 389–395.

McElwain, J. C., and M. Steinthorsdottir. 2017. Paleoecology, ploidy, paleoatmospheric composition, and developmental biology: A review of the multiple uses of fossil stomata. *Plant Physiology* 174: 650–664.

Poole, I., and W. M. Kürschner. 1999. Stomatal density and index: The practice. In T. P. Jones and N. P. Rowe [eds.], Fossil plants and spores, 257–260. The Geological Society, London, United Kingdom.

Porter, A. S., C. Evans-FitzGerald, C. Yiotis, I. P. Montañez., and J. C. McElwain. 2019. Testing the accuracy of new paleoatmospheric CO_2 proxies based on plant stable carbon isotopic composition and stomatal traits in a range of simulated paleoatmospheric O_2:CO_2 ratios. *Geochimica et Cosmochimica Acta* 259: 69–90.

PRISM Climate Group, Oregon State University. 2020. PRISM Climate Data. Website https://prism.oregonstate.edu [accessed October 2022].

Roeske, C. A., and H. O'Leary. 1984. Carbon isotope effects on the enzyme-catalyzed carboxylation of ribulose bisphosphate. *Biochemistry* 23: 6275–6284.

Royer, D. L. 2001. Stomatal density and stomatal index as indicators of paleoatmospheric CO_2 concentration. *Review of Palaeobotany and Palynology* 114: 1–28.

Royer, D. L., L. J. Hickey, and S. L. Wing. 2003. Ecological conservatism in the "living fossil" *Ginkgo*. *Paleobiology* 29: 84–104.

Royer, D. L., K. M. Moynihan, M. L. McKee, L. Londoño, and P. J. Franks. 2019. Sensitivity of a leaf gas-exchange model for estimating paleoatmospheric CO_2 concentration. *Climate of the Past* 15: 795–809.

Rundgren, M., and D. Beerling. 2003. Fossil leaves: Effective bioindicators of ancient CO_2 levels? *Geochemistry, Geophysics, Geosystems* 4: e1058. https://doi.org/10.1029/2002GC000463

Scher, M. A., R. S. Barclay, A. A. Baczynski, B. A. Smith, J. Sappington, L. A. Bennett, S. Chakraborty, et al. 2022. The effect of CO_2 concentration on carbon isotope discrimination during photosynthesis in *Ginkgo biloba*: Implications for reconstructing atmospheric CO_2 levels in the geologic past. *Geochimica et Cosmochimica Acta* 337: 82–94.

Schneider, C. A., W. S. Rasband, and K. W. Eliceiri. 2012. NIH Image to ImageJ: 25 years of image analysis. *Nature Methods* 9: 671–675.

Sheldon, N. D., S. Y. Smith, R. Stein, and M. Ng. 2020. Carbon isotope ecology of gymnosperms and implications for paleoclimatic and paleoecological studies. *Global and Planetary Change* 184: e103060.

Stein, R. A., N. D. Sheldon, and S. Y. Smith. 2024. Comparing methodologies for stomatal analyses in the context of elevated modern CO_2. *Life* 14: e78.

Steinthorsdottir, M., P. E. Jardine, B. H. Lomax, and T. Sallstedt. 2022. Key traits of living fossil *Ginkgo biloba* are highly variable but not influenced by climate – Implications for paleo-pCO_2 reconstructions and climate sensitivity. *Global and Planetary Change* 211: e103786.

Tralau, H. 1968. Evolutionary trends in the genus *Ginkgo*. *Lethaia* 1: 63–101.

von Caemmerer, S. 2000. Biochemical models of leaf photosynthesis. CSIRO, Collingwood, Australia.

SUPPORTING INFORMATION

Additional supporting information can be found online in the Supporting Information section at the end of this article.

Appendix S1. Supplemental tables presenting full data sets, inputs for the Franks model, and ANOVA statistics.

Appendix S2. Supplemental figures comparing results of different preparation methods and different counters.

How to cite this article: Machesky, M. D., N. D. Sheldon, M. T. Hren, and S. Y. Smith. 2025. The sensitivity of reconstructed carbon dioxide concentrations to stomatal preparation methods using a leaf gas exchange model. *Applications in Plant Sciences* 13(1): e11629. https://doi.org/10.1002/aps3.11629